Journal of Photochemistry and Photobiology A: Chemistry 134 (2000) 1–7

Journal of Photochemistry and Photobiology A:Chemistry

www.elsevier.nl/locate/jphotochem

Identification of H-aggregate in a monolayer amphiphilic porphyrin–TiO_2 nanoparticle heterostructure assembly and its influence on the photoinduced charge transfer

J.H. Yang [a,b], Y.M. Chen [b], Y.L. Ren [b], Y.B. Bai [b,*], Y. Wu [c], Y.S. Jang [b],
Z.M. Su [a], W.S. Yang [b], Y.Q. Wang [c], B. Zao [c], T.J. Li [b]

[a] *Institute of Functional Materials Chemistry and Department of Chemistry, Northeast Normal University, Changchun 130024, PR China*
[b] *Department of Chemistry, Jilin University, Changchun 130023, PR China*
[c] *Institute of Theoritical Chemistry, Jilin University, Changchun 130023, PR China*

Received 9 October 1999; received in revised form 14 January 2000; accepted 8 February 2000

Abstract

The spectral properties of the monolayer 5,10,15-tri(4-hydroxyphenyl)-20-(4-hexadecyloxyphenyl) porphyrin molecule (TriHHP)–TiO_2 nanoparticle heterostructure assembly were investigated with absorption, fluorescence emission and excitation spectra, in comparison with those of $CHCl_3$ solution and monolayer films deposited from pH 3 and pH 10 water subphases. A new fluorescence emission band, arising from a blue-shifted Q-absorption band, was observed in the assembly or the monolayer film deposited from pH 3 water subphase. An H-aggregate type species from the protonated TriHHP molecules was assigned to cause this new emission band. According to the Frontier orbital theory, this H-aggregate is suggested in the configuration of face-to-face π–π stacking interaction among the protonated TriHHP molecules. In the heterostructure assembly, the efficient fluorescence emission quenching of TriHHP by the photoinduced charge transfer occurs under excitation in Soret band region of the unprotonated TriHHP molecules. No contribution to the photoinduced charge transfer. © 2000 Elsevier Science S.A. All rights reserved.

Keywords: Monolayer; TriHHP; SOMO–SOMO; SOMO–HOMO

1. Introduction

Organic−inorganic heterostructure has been studied extensively in the fields of electronics and photoelectronics. For the former, it is used mainly for the preparation of rectifying heterojunction competing with the conventional inorganic−inorganic one [1,2]. For the latter, great interest has been gained with regard to photoelectric conversion [3–20]. The surface modification of semiconductors with organic dye molecules can yield efficient charge separation through photoinduced charge injection from the exicited dye molecule into the semiconductor.

It has been recognized that only the first monolayer of dye molecules adsorbed on the surfaces of semiconductors contributes to the efficient charge injection because a direct contact and electronic coupling of the dye molecules with the semiconductor is necessary for the formation of charge transfer channel [21–23]. If more than one monolayer of molecules are adsorbed, the self-quenching effect will reduce the sensitization efficiency dramatically. Therefore, a very important condition for the high efficient photoinduced charge injection is the large adsorption area of the dye molecules on the surface of semiconductor. Nanocrystalline semiconductors distinguish themselves by a high surface-to-volume ratio capable of providing a large dye adsorption area. Some promising researches, based on nanocrystalline TiO_2 electrodes have be obtained [7–9,14,17–19]. Another exciting property of this kind of systems is the high charge transfer rate, which occurs on a pisecond time scale, several orders of magnitude faster than the back-electron transfer. This characteristic would play a key role for a plausible molecular device for photoinduced charge separation [23].

The Langmuir–Blodgett (LB) technique is a good method to fabricate two-dimensionally ordered arrays of semiconductor nanoparticle quantum dots by using nanoparticle semiconductor hydrosols as the subphase [24–27]. Therefore, amphiphilic dye molecules may be approved to be used in fabricating the ordered arrays of monolayer

---

* Corresponding author. Fax: +86-431-8923907.
E-mail address: yubai@mail.jlu.edu.cn (Y.B. Bai)

1010-6030/00/$ – see front matter © 2000 Elsevier Science S.A. All rights reserved.
PII: S1010-6030(00)00239-2

dye-semiconductor heterostructure assembly on molecular level by this technique. In a previous paper [28], we preliminarily reported the monolayer characteristics of 5,10,15-tri(4-hydroxyphenyl)-20-(4-hexadecyloxyphenyl) porphyrin (TriHHP) on the surfaces of water and TiO_2 hydrosol subphases (both pH 3) through surface pressure–area isotherms, and the UV–Vis absorption characteristics of the deposited monolayers. It was proven that the monolayer porphyrin molecule–TiO_2 nanoparticle heterostructure assembly could be formed. In the present paper, we investigate in detail the absorption, fluorescence emission and excitation properties of TriHHP in this heterostructure assembly in comparison with monolayers deposited from pH 3 and 10 water subphases, and its $CHCl_3$ solution. An H-aggregate type of species was identified in this assembly, coming from the protonated TriHHP molecules. According to the Frontier orbital theory [29,30], its formation mechanism is suggested. This kind of H-aggregate was found to contribute less to the photoinduced electron injection to TiO_2 nanoparticle.

2. Experimental

TriHHP, a amphiphilic molecule with the hydroxyl group as the hydrophilic part and the long hydrocarbon chain as the hydrophobic part (Scheme 1), was synthesized according to the following procedure: Na_2CO_3 (0.35 g, 5 mmol) was added to solution of 5,10,15,20-Tatre(4-hydroxyphenyl) porphyrin (1.356 g, 2 mmol) in THF (20 ml) under stirring, then solution of 1-bromohexadecane (0.61 g, 2 mmol) in THF(10 ml) was added and the resulting mixture was refluxed for 10 h. The resulting solution was carefully neutralized at room temperature with 10% HCl, and then extracted with DMF. The extract was washed with water, concentrated and dried in vacuum. The dark residue was purified by column chromatograph on silica gel, using a mixture of THF and $(CH_2)_2Cl_2$ (1/2, v/v) as eluent. TiO_2 hydrosol was prepared following the method described by C. Kormann [31]. Details about the characteristics of the materials, conditions and procedure for the preparation of the TriHHP monolayer from water subphase (pH 3) and the monolayer TriHHP$-$$TiO_2$ nanoparticle heterostructure assembly from TiO_2 hydrosol subphase have been given in Ref. [28].

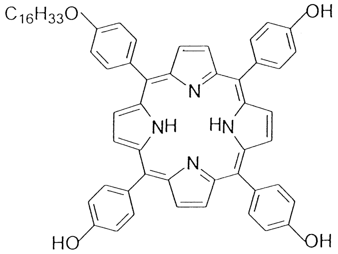

Scheme 1. Structure of 5,10,15-tri(4-hydroxyphenyl)-20-(4-hexadecyloxyphen-yl)porphyrin (TriHHP).

For comparison study, the surface pressure-area (π-A) isotherm of TriHHP monolayer on the surface of pH 10 water subphase (adjusted by addition of NaOH), the absorption, fluorescence, and excitation spectra of the monolayer deposited onto a cleaned CaF_2 substrate were studied. The film compression and deposition conditions were the same with those in the pH 3 water and TiO_2 subphases.

The UV–Vis absorption spectra of the deposited films were measured with a Shimadzu UV-3100 spectrometer (Japan). The fluorescence emission and excitation spectra were measured on a Spex 1902 Fluorolog with a 450 W xenon lamp as excitation source. All the measurements were conducted at room temprature, ca. 21°C. To ensure species dynamic equilibration, all the prepared samples were kept in the dark for 24 h prior to spectral measurements.

3. Results and discussion

3.1. Partly-protonated effect of TriHHP in the monolayer and heterostructure assembly

The π-A isotherms of TriHHP monolayers on the surfaces of the pH 3 water and TiO_2 hydrosol subphases have been discussed in Ref. [28]. The π-A isotherms of TriHHP monolayers on the surfaces of pH 3 (a) and 10 (b) water subphases are shown in Fig. 1. On the surface of pH 3 water subphase, the TriHHP monolayer has smaller surface pressure-beginning area and extrapolated molecular area than on the surface of a pH 10 water subphase.

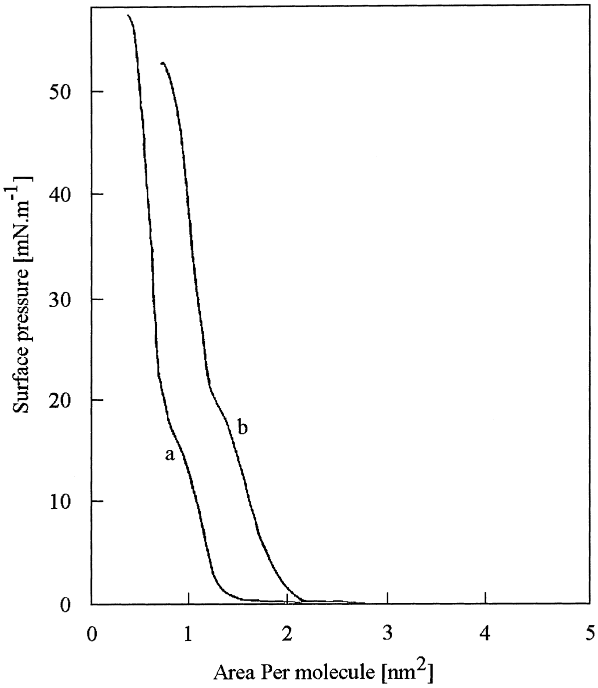

Fig. 1. The surface pressure-area (π-A) isotherms of TriHHP monolayers on the surfaces of pH 3 water (a) and pH 10 water (b) subphases.

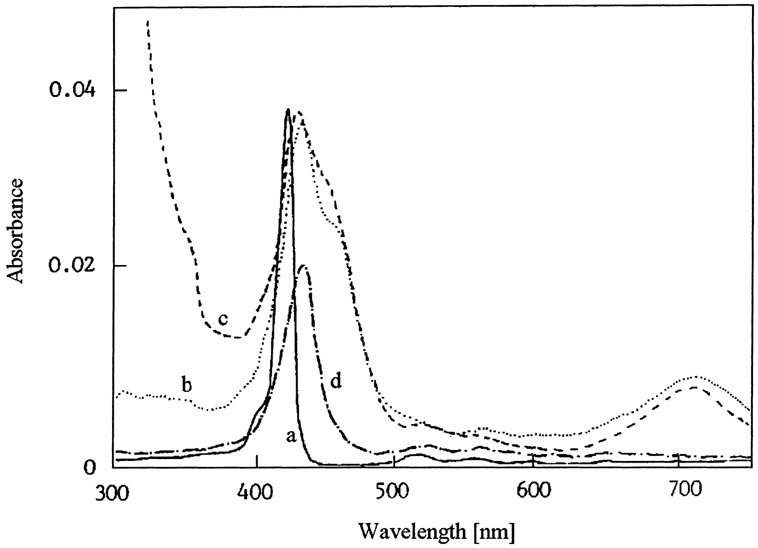

Fig. 2. The absorption spectra of TriHHP in 2.0×10^{-4} M $CHCl_3$ solution (a), monolayer films deposited from pH 3 water (b), pH 3 TiO_2 hydrosol (c) and pH 10 water (d) subphases.

The absorption spectra of TriHHP in $CHCl_3$ solution (a), monolayer films deposited from pH 3 water (b), TiO_2 hydrosol (c), and pH 10 water (d) subphases are shown in Fig. 2 Marking the absorption of TriHHP free base, the solution spectrum is characterized by a Soret absorption band at 420 nm, and four split weak Q absorption bands at ca. 520, 560, 600, and 650 nm. The Soret absorption peak of TriHHP in the monolayer film deposited from pH 3 water subphase is broadened and red-shifted to 433 nm. The monolayer TriHHP–TiO_2 nanoparticle heterostructure assembly has a strong absorption band of TiO_2 nanoparticle in the UV region ($\lambda<380$ nm).

It can be seen that the two extra bands at ca. 460 nm (shoulder) and 710 nm in Fig. 2b disappear in the absorption spectrum of TriHHP monolayer deposited from pH 10 water subphase. Thus, they can be attributed to the characteristic absorption of the protonated TriHHP. However, there is not evidence that a J-aggregate of the protonated TriHHP molecules is formed because of the lack of the more red-shifted, sharp absorption band at ca. 490 nm [32–36]. The position of the Soret absorption peak of a monolayer deposited from pH 3 water subphase is essentialy the same with that of a monolayer deposited from a pH 10 water subphase, showing that this Soret absorption peak is mainly from the unprotonated TriHHP molecules. The spectral characteristic of TriHHP molecules in the heterostructure assembly, is similar to that in the monolayer film from pH 3 water subphase, except for the whole blue-shifted effect due to the electronic coupling of TriHHP with TiO_2 nanoparticle [28].

3.2. An H-aggregate type species of TriHHP in the heterostructure assembly

Fig. 3a gives the fluorescence emission spectrum of TriHHP in $CHCl_3$ solution (2.0×10^{-4} M). Under excitation in the Soret or Q-band region (not shown), only one fluorescence emission process occurs, centering at about 659 nm. However, shown in Fig. 3b, the fluorescence emission spectrum of TriHHP in an assembly, has a dramatic deviation from the solution spectrum. Besides the fluorescence emission band of the unprotonated TriHHP molecules (free base) at ca. 663 nm corresponding to that at 659 nm in the solution spectrum, there still exists a new fluorescence emission band in the shorter wavelength region. TiO_2 nanoparticles can not be photoexcited by the 420 nm light, and a completely same phenomenon is also observed in the fluorescence emission spectrum of TriHHP monolayer film from pH 3 water

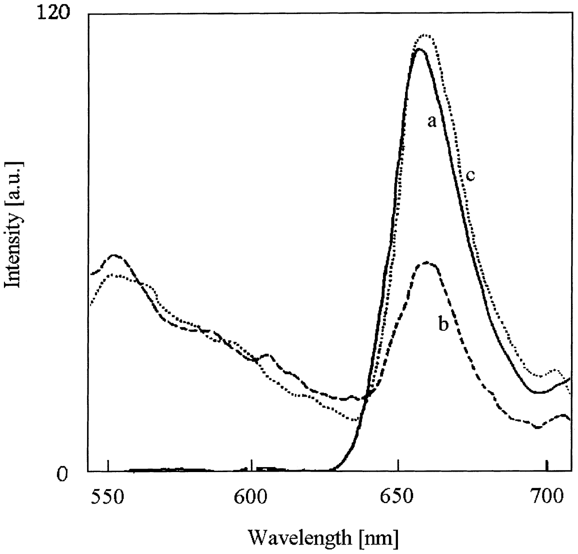

Fig. 3. The fluorescence emission spectra of TriHHP in 2.0×10^{-4} M $CHCl_3$ solution (a), the heterostructure assembly (b), and the monlayer (c). Excitation wavelength: 420 nm.

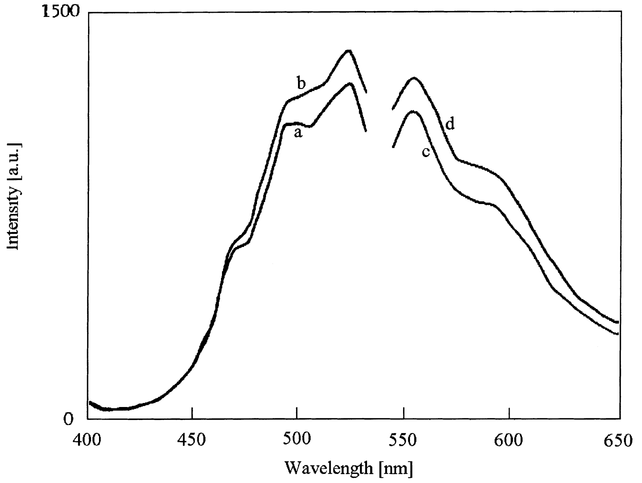

Fig. 4. The fluorescence excitation and emission spectra of the new species of TriHHP in the heterostructure assembly (a and c) and monolayer film (b and d) at $\lambda_{em}=554$ nm and $\lambda_{ex}=520$ nm, respectively.

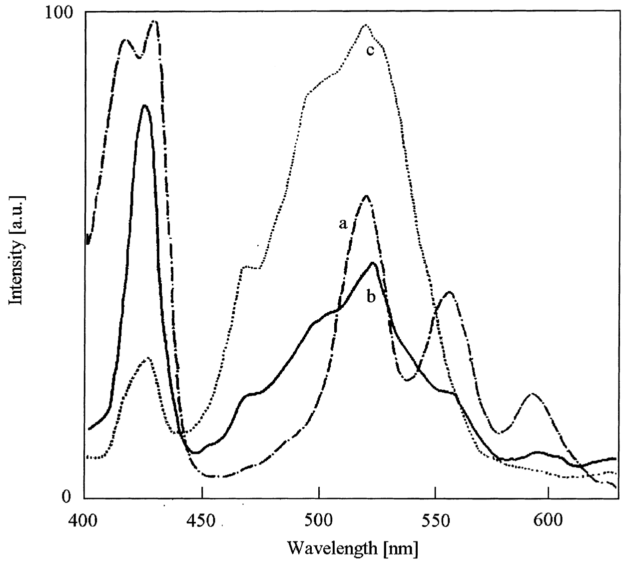

Fig. 5. The fluorescence excitation spectra of TriHHP in $CHCl_3$ solution (a), the monolayer film (b) and the heterostructure assembly (c) at $\lambda_{em}=663$ nm.

subphase (see Fig. 3c). So this new fluorescence emission band implies a new species of TriHHP in the assembly, only related to the properties of TriHHP itself rather than the interaction between TriHHP and TiO_2 nanoparticle.

The fluorescence excitation spectra of the new species of TriHHP in the assembly and monolayer film were measured at $\lambda_{em}=554$ nm. As displayed in Fig. 4(a or b), an absorption band, with distinctive fine structures and considerably blue-shifted with respect to the blue-most absorption band of the solution, is detected in the range of 450–520 nm. Fig. 4(c or d) shows a good mirror-image relation between the new fluorescence emission band ($\lambda_{ex}=520$ nm) and its excitation band. The fluorescence excitation spectra of TriHHP in $CHCl_3$ solution (a), the monolayer film (b) and heterostructure assembly (c) at $\lambda_{em}=663$ nm are displayed in Fig. 5. Compared with the $CHCl_3$ solution, the monolayer film or heterostructure assembly has an obviously blue-shifted part in the absorption region of Q band, which is in coincidence with the fluorescence excitation spectrum in Fig. 4.

Fig. 6 give the emission and excitation spectra of a monolayer deposited from a pH 10 water subphase. With the disapper of this new emission band and the blue-shifted Q absorption band, the emission and excitation spectra have similar spectral characteristics with those of the $CHCl_3$ solution, respectively. The same acidity is the only common property of pH 3 TiO_2 hydrosol and pH 3 water subphases from which the assembly and the monolayer film are deposited, respectively. Therefore, the protonated TriHHP molecules results in the formation of the new species.

The monomer of a protonated porphyrin molecule has its absorption region red-shifted relative to the porphyrin free base [33–36]. Akins and others found that protonated meso-tetrakis(*p*-sulfonatophenyl)porp(yrin ($H_4^{2+}TSPP^{4-}$) in an acidic solution can give rise to a J-aggregate type arrangement in a cofacial fashion with a displacement between the oppositely charged sites, due to the strong electrostatic interaction [32,34–36]. In the case of the protonated TriHHP molecules, the electrostatic interaction between the oppositely charged sites is not present due to the lack of negative charge groups, and the J-aggregate type species from the protonated TriHHP can not be found. Instead, the blue-shifted Q absorption band shows the existence of the new species in an H-aggregate type arrangement.

Arising from protonation effect, the charge density on the pyrrolic N was reduced under the attachment of the H^+ with the emptied 1 s orbital. Consequently, the protonated N atom prefers to draw electron from the HOMO (a_{2u} orbital) of the

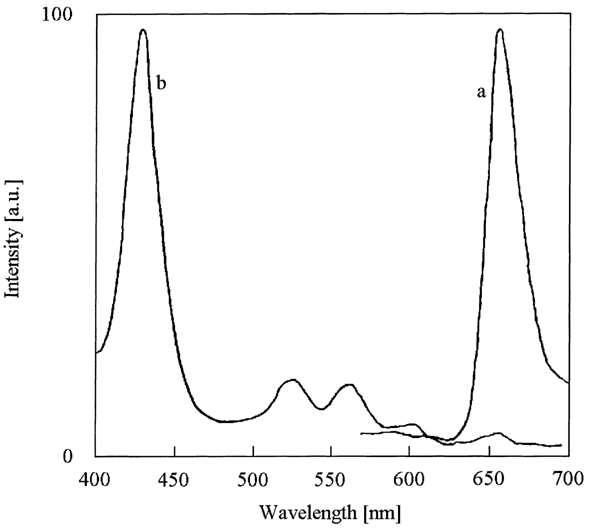

Fig. 6. The emission (a) and excitation (b) spectra of the monolayer deposited from pH 10 water subphase at $\lambda_{ex}=420$ nm and $\lambda_{em}=663$ nm.

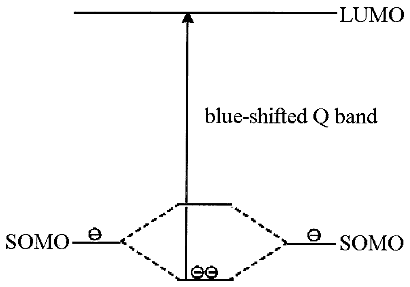

Fig. 7. A simple schematic of the face-to-face π–π stacking interaction suggestd for the formation of the H-aggregate type species of the protonated TriHHP molecules.

porphyrin ring [36], i.e., the protonated TriHHP molecule becomes π active due to the partial lose of electron in the HOMO. According to the Frontier orbital theory [29,30], aggregation among the protonated TriHHP molecules whose HOMO becoming partially electron-occupied (to simplify, it is supposed to be singly occupied molecular orbital SOMO), or aggregation between protonated TriHHP molecules and unprotonated ones, may happen by a face-to-face π–π stacking interaction (SOMO–SOMO or SOMO–HOMO interaction) to form a stable aggregated species that will bring a higher stability of the whole system. Considering the number of stabilized electrons, and the steric hindrance effect of the peripheral meso-substituted phenyl groups of the unprotonated porphyrin which are generally in a perpendicular orientation to the macrocycle [34,37], the SOMO–SOMO interaction seems to be more practical. Fig. 7 is a simple schematic of this type of π–π interaction. The kind of π–π interaction would result in a lower bonding MO, and hence a higher transition energy from this MO to the LUMO corresponding to a blue-shifted Q absorption band. Akins et al. have ascertained that without the interaction between $H_4^{2+}TSPP^{4-}$ and H_2TSPP^{4-} molecules, the J-aggregates were formed among protonated $H_4^{2+}TSPP^{4-}$ molecules due to the significantly smaller steric hindrance between them, which arises from the induced twisting from the near perpendicular orientation of the meso-substituted aryl groups to an essentially coplanar conformation relative to the mean plane of the macrocycle by the protonation effect [34–36]. In the same way, this reorientation of the meso-aryl substituents is expected to significantly reduce the steric hindrance and favors the effective SOMO–SOMO interaction between the neighboring macrocycles of the protonated TriHHP molecules, although the Coulombic repulsive force between positively charged macrocycles [35]. The absorption and Raman spectra of H_2TSPP^{4+} acidic solution show that although J-aggregate is formed mainly, there still be a small amount of H-aggregate of the protonated H_2TSPP^{4+} molecules [34]. Recently, it has been reported that 5,10(or 5,15)-diphenyl-15,20(or 10,20)-bis[4-(*N*-methyl)pyridinium] porphyrin cations can be dimerized by the π–π stacking interaction [38]. These facts exhibit that the special molecular structure and environment play an essential role in determining the formation mode of the aggregate from protonated porphyrin molecules. In our system, the three hydrophilic hydroxyls and the hydrophobic hydrocarbon chain make the protonated TriHHP molecule polarized and orientated (solvophobic), even probably hydrogen-bond interacting. All of these are working for an effective face-to-face π–π stacking interaction between protonated TriHHP molecules. Returning to Fig. 1, the surface pressure-beginning area of TriHHP monolayer on the surface of a pH 3 water subphase is smaller than on the surface of a pH 10 water subphase. It gives the verification of the formation of aggregate in the monolayer on the surface of a pH 3 water subphase.

In discussion above, we did not deal with the Soret absorption of this H-aggregate type species. From Fig. 3, it is known that under the excitation at $\lambda_{ex}=420$ nm, the emission band of this H-aggregate type species occurs accompanying the emission band of unprotonated TriHHP molecules (at ca. 663 nm). It reveals that the Soret absorption of this H-aggregate type species is mixed with the Soret absorption band of unprotonated TriHHP molecules. As shown in Fig. 2(b and c), although unobviously, the Soret absorption peak and its blue region seem to be overlapped.

3.3. Photoinduced electron transfer from porphyrin to TiO_2

From Fig. 3, one can see that 663 nm fluorescence emission band of unprotonated TriHHP molecules in the assembly decreases pronouncedly, in contrast to the monolayer film. In the fluorescence excitation spectrum of TriHHP in the assembly at $\lambda_{em}=663$ nm in Fig. 5, the relative intensity of the Soret absorption band to that of the Q absorption band is drastically low, in comparison with the TriHHP monolayer film or $CHCl_3$ solution. It implies a considerable decrease of the contribution of the Soret band absorption to the 663 nm fluorescence emission band. Because of the higher absorption threshold (about 380 nm) than the Soret absorption energy of TriHHP, TiO_2 nanoparticles would not cause the decrease of the contribution of the Soret band absorption of TriHHP in the assembly to such a great extent. In fact, showing insignificant influence of TiO_2 nanoparticle on the absorption intensity of TriHHP, Fig. 2 shows that TriHHP in the assembly has essentially the same absorption intensity as it has in the monolayer film. Thus, the pronounced decreases of the 663 nm fluorescence emission band of unprotonated TriHHP molecules in the assembly exhibits fluorescence emission quenching, i.e., after excited with lightin the Soret band region, a rather amount of unprotonated TriHHP molecules can not irradiate back to the ground state.There are two possible pathways for the fluorescence emission quenching of dye molecules adsorbed on the surface of TiO_2 [17]: concentration self-quenching among the dye molecules or photoinduced electron transfer from the excited dye molecule to the conduction band (or an acceptor surface state) of TiO_2. In this assembly, it cannot be excluded that the small intermolecular distance would result in energy transfer quenching the emission. But we hold that this kind of quenching mechanism is not the only or main reason for the observed fluorescence emission quenching at 663 nm. In Fig. 3, the TriHHP monolayer film has strong fluorescence emission under excitation in the Soret absorption band. And furthermore, probably implying the same extent of influence of the aggregation effect on the fluorescence emission and excitation for both systems, Fig. 4. shows the emission band or the corresponding blue-shifted Q absorption band of the H-aggregate species in the assembly has essentially the same shape and intensity with that in a monolayer film. We consider therefore that the photoinduced electron transfer from $e_g(\pi^*)$ of the excited TriHHP molecule to TiO_2 nanoparticle is operative for the significant fluorescence emission quenching. In fact, it has been known that TiO_2 nanoparticle can trap rapidly and highly efficiently an electron from a photoexcited porphyrin and other organic dye molecules [14,17,18].

Photoinduced electron transfer requires an effective energetic match and electronic coupling between the dye molecule and the modified semiconductor. The observed photoinduced electron transfer from unprotonated TriHHP to TiO_2 shows further the good electronic coupling between them, which ensures the formation of the heterostructure and its transfer onto CaF_2 substrates.

As far as the new emission or excitation bands of the H-aggregate from protonated TriHHP molecules in the assembly is concerned, no fluorescence emission quenching or obvious decrement of absorption could be observed. It means that the blue-shifted Q band excitation of this H-aggregate has little contribution to the photoinduced electron transfer to TiO_2 nanoparticle. The same conclusion can be obtained for the Soret excitation of this H-aggregate because of the unchanged intensity of the new emission band (see Fig. 3). We infer that there perhaps are two reasons for it. The first is that the electron photoexcited to $e_g(\pi^*)$ orbital has too short lifetime to transfer efficiently to TiO_2 nanoparticle, because of a strong intermolecular electronic interaction in the aggregated species [17,36]. The second is that this H-aggregate is charged as the electron-deficient species, and hence the coulombic repulsion may preclude its effective adsorption on the surface of TiO_2 nanoparticle, in another words, the effective electronic coupling of its $e_g(\pi^*)$ wave function with the 3d orbital of Ti^{4+} (or surface state) of TiO_2 nanoparticle is not meet, which is unfavorable for the formation of charge transfer channel.

The formed H-aggregate of TriHHP in the assembly arises from the protonation effect. Considering the lack of contribution of it to the photoinduced electron transfer, it seems reasonable to increase the pH value of the TiO_2 hydrosol subphase for assembly preparation, in order to decrease the formation probability of this kind of H-aggregate. Of course, this should be carried out under the premise of stable TiO_2 nanoparticle as well as good assembly quality. The related work should be developed further.

4. Conclusion

Recent studies show that nanocrystalline TiO_2, affords rather favorably molecular device for photoinduced charge separation. In this paper, we studied the spectral properties of the two-dimensionally ordered arrays of monolayer 5,10,15-tri(4-hydroxyphenyl)-20-(4-hexadecyloxyphenyl) porphyrin (TriHHP) molecule–TiO_2 nanoparticle heterostructure assembly. An H-aggregate type species of the protonated TriHHP in the assembly was found. According to the Frontier orbital theory, this H-aggregate is suggested existing in the forms of a face-to-face π–π stacking among the protonated TriHHP molecules. Fluorescence emission quenching by a photoinduced charge transfer to TiO_2 nanoparticle was observed under the excitation in Soret band region of the unprotonated TriHHP molecules. No charge transfer from this H-aggregate to TiO_2 nanoparticle could be observed in the assembly.

References

[1] F.F. So, S.R. Forest, J. Appl. Phys. 63 (1988) 442.
[2] L. Ottaviano, S. Santucci, S. Di Nardo, L. Lozzi, M. Passacantando, P. Picozzi, J. Vac. Sci. Technol. A 15 (1997) 1014.
[3] T. Miyasaka, T. Watanabe, A. Fujishima, K. Honda, Nature 277 (1979) 638.
[4] P.K. Gosh, T.G. Spiro, J. Am. Chem. Soc. 102 (1980) 5543.
[5] M. Motsumura, K. Mitsuda, N. Yoshizawa, H. Tsubomura, Bull. Chem. Soc. Jpn. 54 (1981) 692.
[6] A.P. Hong, D.W. Bahneman, M.R. Hoffman, J. Phys. Chem. 91 (1987) 2109.
[7] K. Kalyanasundaram, N. Vlachopoulos, V. Krishnan, A. Monnier, M. Gratzel, J. Phys. Chem. 91 (1987) 2342.
[8] E. Vrachnou, N. Vlachopouls, M. Gratzel, J. Chem. Soc. Chem. Commun. 1987 868.
[9] B. O' Regan, M. Gratzel, Nature 353 (1991) 737.
[10] M. Hiramoto, H. Fukusumi, M. Yokoyama, Appl. Phys. Lett. 61 (1992) 2580.
[11] R. Amadelli, M. Bregolu, E. Polo, V. Carassiti, A. Maddotti, J. Chem. Soc. Commun. 1992 1355.
[12] M.K. Nazeruddin, A. Kay, I. Rodicio, R. Humphry-Baker, E. Muller, P. Liska, N. Vlachopoulos, M. Gratzel, J. Am. Chem. Soc. 115 (1993) 6382.
[13] A. Kay, M. Gratzel, J. Phys. Chem. 97 (1993) 6272.
[14] J. Moser, M. Gratzel, Chem. Phys. 176 (1993) 493.
[15] A. Kay, R. Humphry-Baker, M. Gratzel, J. Phys. Chem. 98 (1994) 952.
[16] K. Koyama, N. Yamaguchi, T. Miyasaka, Science 265 (1994) 762.
[17] R.F. Khairutdinov, N. Serpone, J. Phys. Chem. 99 (1995) 11952.
[18] S.Y. Huang, G. Schlichthorl, A.J. Nozik, M. Gratzel, A.J. Frank, J. Phys. Chem. B 101 (1997) 2576.
[19] G. Schlichthorl, S.Y. Huang, J. Sprague, A.J. Frank, J. Phys. Chem. B 101 (1997) 8141.
[20] J.H. Yang, J. Zhang, D.J. Wang, Y.B. Bai, H.R. Sun, D.F. Shen, T.J. Li, J. Photochem. Photobiol. A 112 (1998) 225.
[21] N. Vlachopoulos, P. Liska, J. Augustyniski, M. Gratzel, J. Am. Chem. Soc. 110 (1988) 1216.
[22] T.A. Heimer, C.A. Bibnozzi, G.T. Meyer, J. Phys. Chem. 97 (1993) 11987.
[23] A. Hagfeldt, M. Gratzel, Chem. Rev. 95 (1995) 49.
[24] X.G. Peng, Y. Zhang, B.S. Zou, L.Z. Xiao, T.J. Li, J. Yang, J. Phys. Chem. 96 (1992) 3412.

[25] F.C. Meldrum, N.A. Kotov, J.H. Fendler, Langmuir 10 (1994) 2035.
[26] T. Nakaya, Y. Li, K. Shibato, J. Mater. Chem. 6 (1996) 691.
[27] M. Sastry, K.S. Mayya, V. Patil, D.V. Paranjape, S.G. Hegde, J. Phys. Chem. B 101 (1997) 4954.
[28] J.H. Yang, Y.M. Chen, Y.B. Bai, Y. Wu, W.Q. Xue, M. Xan, D.F. Shen, Y.Q. Wang, S.R. Du, R. Lu, T. Li, J. Porphyrin-TiO_2 nanoparticle heterostructure assembly by Langmuir-Blodgett method. Supramole. Sci., in press.
[29] H. Fujimoto, K. Fukui, in: H. Ratajczak, W.J. Orville-Thomas (Eds.), Molecular Interactions, Wiley, New York, 1980 p. 89.
[30] C. Hunter, J.K.M. Sanders, J. Am. Chem. Soc. 112 (1990) 5525.
[31] C. Komann, D.W. Bahnemann, M.R. Hoffmann, J. Phys. Chem. 92 (1988) 5196.
[32] O. Ohno, Y. Kaizu, H. Kobayashi, J. Chem. Phys. 99 (1993) 4128.
[33] M.B. Grieve, A.J. Hudson, T. Richardson, R.A.W. Johnstone, A.J.F.N. Sobral, A.M.d'A. Rocha Gonsalves, Thin Solid Films 243 (1994) 581.
[34] D.L. Akins, H.R. Zhu, C. Guo, J. Phys. Chem. 98 (1994) 3612.
[35] D.L. Akins, H.R. Zhu, C. Guo, J. Phys. Chem. 100 (1996) 5420.
[36] D.L. Akins, S. Ozcelik, H.R. Zhu, C. Guo, J. Phys. Chem. 100 (1996) 14390.
[37] A. Stone, E.B. Fleischer, J. Am. Chem. Soc. 90 (1968) 2735.
[38] K. Kano, H. Minamizono, T. Kitae, S. Negi, J. Phys. Chem. A 101 (1997) 6118.